Electronic states of single crystal $CeAl_2$ near the pressure-induced quantum critical point

Hidenori Miyagawa and Gendo Oomi
Department of Physics, Kyushu University, Ropponmatsu, Chuo-ku, Fukuoka 810-8560, Japan

Masashi Ohashi
Faculty of Environmental Design, Kanazawa University, Kanazawa, Ishikawa 920-1192, Japan

Isamu Satoh
Institute for Materials Research, Tohoku University, Sendai 980-8577, Japan

Takemi Komatsubara
Center for Low Temperature Science, Tohoku University, Sendai 980-8577, Japan

Masato Hedo
Faculty of Science, University of the Ryukyus, Nishihara, Okinawa 903-0213, Japan

Yoshiya Uwatoko
Institute for Solid State Physics, University of Tokyo, Kashiwa, Chiba 277-8581, Japan
(Received 25 February 2008; revised manuscript received 29 May 2008; published 5 August 2008)

The electrical resistivity and magnetoresistance (MR) of single crystal $CeAl_2$ have been measured up to 8 and 3.2 GPa, respectively. The magnetic part of the electrical resistivity ρ_{mag} increases as temperature decreases until it shows two maxima around 5 K($=T_1$) and 63 K($=T_2$) at ambient pressure. As pressure increases, T_1 and T_2 decrease up to 2 and 3 GPa, respectively, but they begin to increase above these pressures. MR changes from negative to positive with increasing pressure. It is suggested that Kondo temperature T_K increases as pressure increases. Above 3 GPa, Fermi-liquid behavior obeying T^2 dependence of the electrical resistivity is observed and the coefficient of T^2 dependence diverges around 2.7 GPa. The Néel temperature of $CeAl_2$ at ambient pressure is 3.8 K($=T_N$) and it is suppressed to zero around 2.7 GPa. In the pressure range of 2.5 GPa$\leq P \leq$2.7 GPa, $\rho_{mag}(T)$ deviates largely from the normal Fermi-liquid behavior, which suggests the so-called non-Fermi-liquid behavior around 2.7 GPa. Pressure-induced superconductivity was not observed down to 50 mK around 2.7 GPa.

DOI: 10.1103/PhysRevB.78.064403 PACS number(s): 75.20.Hr, 73.43.Nq, 74.62.Fj

I. INTRODUCTION

The $4f$ electrons in Ce compounds have been well known as showing various interesting physical properties such as magnetic ordering, valence fluctuation, heavy fermion owing to competition between the Ruderman-Kittel-Kasuya-Yoshida (RKKY) interaction, and Kondo effect.[1,2] The former interaction enhances a magnetic ordered state and the $4f$ electron is treated as a localized one. The latter gives rise to a screening of the $4f$ local moment by the conduction electrons and leads to the itinerant nonmagnetic state. It has been well known that RKKY interaction and Kondo effect are sensitive to pressure.[3] Through the investigation under high pressure, we can get a lot of useful information about the mechanism of Kondo or heavy fermion states.

In several Ce compounds, the unconventional physical properties have been observed around quantum critical point (QCP) which is the point that the ordering temperature is tuned to zero by adjusting a control parameter such as high pressure or chemical composition and so on.[4–6] Around QCP, the anomalous temperature dependence of the specific heat and the resistivity, which deviate strongly from normal Fermi-liquid behavior, have been observed. This is called as non-Fermi-liquid behavior. On the other hand, Fermi-liquid behavior is recovered in the nonmagnetic region obtained by changing parameter further across QCP. Until now, we have reported several examples showing QCP in Ce compounds by measuring the electrical resistivity under high pressure.[7–10]

$CeAl_2$ with the cubic Laves phase $MgCu_2$ structure is well known as a typical heavy fermion compound, which has the large electronic specific-heat coefficient $\gamma = 135$ mJ/mol K^2.[11] Antiferromagnetic order is observed at $T_N = 3.8$ K,[12–15] which is due to the formation of spin-density wave (SDW). The Ce ion in $CeAl_2$ is trivalent at ambient pressure. Kondo temperature T_K and the crystal electric field (CEF) splitting energies were estimated to be 6 K, $\Delta_1 = 100$ K, and $\Delta_2 = 180$ K from the neutron-scattering measurement.[11,16] Although the CEF of cubic Ce compounds should split the $J=5/2$ ground state into a Γ_7 doublet and a Γ_8 quartet, the CEF splitting in $CeAl_2$ shows three levels. This was explained by assuming an existence of bound state between a crystal-field excitation and a low-lying phonon by strong magnetoelastic coupling.[17]

Electrical resistivity under high pressure has been reported by several authors.[7,8,18,19] T_N decreases with increasing pressure. T_K increases as pressure increases and the magnitude of CEF splitting decreases with increasing pressure.[7,18] T^2 dependence in electrical resistivity which is a characteristic of Fermi-liquid behavior was observed above 3

GPa. The coefficient A of T^2 term diverges around 3 GPa, which suggests an existence of QCP around 3 GPa. The electrical resistivity at various temperatures was measured up to 13 GPa by using quasihydrostatic pressure,[19] but details of the electronic states have not been reported.

In the present work, we have measured the electrical resistivity up to 8 GPa and magnetoresistance (MR) up to 3.2 GPa to examine the stability of Kondo or heavy fermion states of $CeAl_2$ by controlling the competition between RKKY interaction and Kondo effect using high pressure. Since T_N is decreased by applying pressure, we made an attempt to induce QCP at high pressure to look for the development of different ground states such as superconductivity or non-Fermi-liquid state by carrying out the detailed analysis of the electrical resistivity.

II. EXPERIMENTAL METHOD

Single crystals of $CeAl_2$ and $LaAl_2$ were grown by Czochralski pulling method with the typical size of 5 mm in diameter and 50 mm in length. The electrical resistivity was measured with the applying current parallel to the a axis in the temperature range between 2 and 300 K by a standard four-probe method using copper wires (diameters 50 μm) or gold wires (diameters 20 μm). Hydrostatic pressures up to 3.2 and 8.0 GPa were generated using a piston-cylinder device[20] and a cubic anvil device,[21] respectively. A 1:1 mixture of Fluorinert, FC70, and FC77 was used as a pressure transmitting medium. The pressure inside the cell was kept constant in all temperature ranges in the present work by automatic controlling of the load. The electrical resistivity around 3 GPa down to 50 mK was measured by means of dilution refrigerator and clamp-type pressure cell. The magnetic field was applied perpendicularly to the current direction up to 9 T.

III. EXPERIMENTAL RESULTS

A. Kondo scattering under high pressure

Figure 1(a) shows the temperature dependent electrical resistivity $\rho(T)$ of $CeAl_2$ at various pressures and nonmagnetic $LaAl_2$ at ambient pressure for comparison. At ambient pressure, $\rho(T)$ of $CeAl_2$ decreases with decreasing temperature and shows a peak around 5 K and a shoulder around 60 K. The peak shifts to lower temperature and disappears above 2.5 GPa. On the other hand, the shoulder is enhanced at high pressure becoming a broad peak centered around 50 K at 3 GPa. The broad peak becomes less prominent by applying higher pressure.

The magnetic part of electrical resistivity $\rho_{mag}(T)$ was estimated by subtracting phonon contribution using the $\rho(LaAl_2)$, $\rho_{mag}(T)=\rho(CeAl_2)-\rho(LaAl_2)$, where we assume that the phonon part of $\rho(CeAl_2)$ is approximated by $\rho(LaAl_2)$. $\rho_{mag}(T)$ curves are shown in Fig. 1(b) as a function of temperature in the logarithmic scale. T_N at ambient pressure was shown by an arrow. $\rho_{mag}(T)$ at ambient pressure has two maxima due to combination of Kondo effect and CEF splitting, which were observed up to 2.4 GPa. These peaks become a single peak above 2.5 GPa through a shoulder in

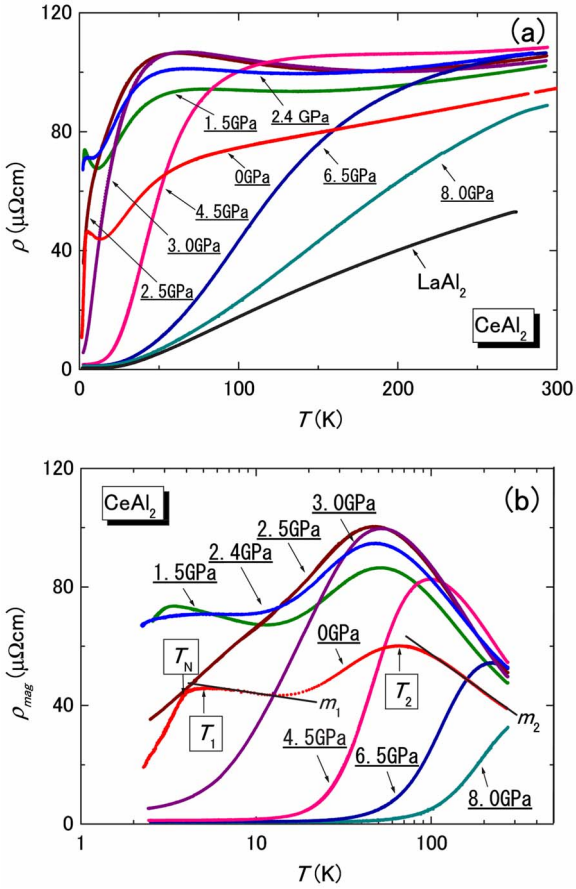

FIG. 1. (Color online) (a) Temperature dependence of the electrical resistivity under high pressure. (b) The temperature dependence of ρ_{mag}. T_N at ambient pressure was shown by an arrow. T_1 and T_2 show the temperature of two maxima.

the $\rho(T)$ around 2.5 GPa. $\rho_{mag}(T)$ is found to show $-\log T$ dependence characteristic to Kondo effect in the temperature ranges 7 K$\leq T\leq$20 K and 100$\leq T\leq$300 K. The coefficients of $-\log T$ are defined to be m_1 and m_2 as shown in Fig. 1(b). Figure 2(a) shows the pressure dependence of T_1, T_2, and T_N. Here, T_1 and T_2 were determined by the temperature dependence of first derivative of $\rho_{mag}(T)$ as the temperatures of $d\rho_{mag}/dT=0$, which are shown in Fig. 2(b). Above 2.4 GPa, a shoulder in $d\rho_{mag}/dT$ is still observed around 10 K up to 2.7 GPa. The temperature showing shoulder T_s was defined as the minimum or the point showing a sudden increase of $d\rho_{mag}/dT$. T_s [shown by the triangle in Fig. 2(a)] is found to fall on the curve extrapolated from low pressure and shifts to higher temperature as pressure increases. It is interesting to note that $\rho_{mag}(T_2)$ increases below 2.5 GPa with pressure, while it decreases above 2.5 GPa. It is found that T_2 decreases with pressure below 3 GPa, but begins to increase above 3 GPa. The similar behavior for T_1 and T_2 has been reported in other Ce compounds such as $CeCu_2Si_2$ and $CeCu_2Ge_2$.[4,22] The details of this pressure effect will be discussed later.

Figure 3 shows ρ_{mag} above 2.5 GPa as a function of T^2. Above 3 GPa, T^2 dependent electrical resistivity is observed below 10–20 K. This means that Fermi-liquid state is stable above 3 GPa and stabilized more as pressure increases since

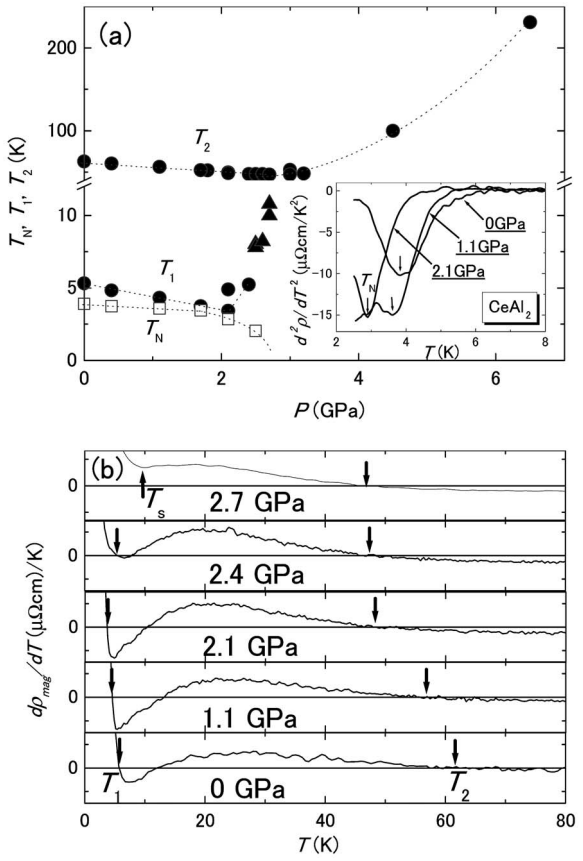

FIG. 2. (a) T_1, T_2, and T_N as a function of pressure. The closed circles show the pressure dependence of T_1 and T_2, and the closed triangles show that of the temperature where a shoulder is observed in $d\rho_{mag}/dT$. The open squares show T_N as a function of pressure. The dashed line is a guide to the eyes. Second derivative of $\rho(T)$ at high pressures is shown in the inset as a function of temperature. (b) The temperature dependence of first derivative of $\rho_{mag}(T)$. The arrows show T_1, T_2, and T_S. Here, T_1 and T_2 were determined as the temperatures of $d\rho_{mag}/dT=0$, and T_s was determined as the temperature showing a minimum of $d\rho_{mag}/dT$.

the temperature range showing T^2 dependence increases with pressure. The pressure dependence of the coefficient A of T^2 term is shown in Fig. 4. A decreases rapidly as pressure increases and seems to diverge around 3 GPa. The previous data in $CeAl_2$ are plotted also in Fig. 4.[7]

B. Effect of pressure on the antiferromagnetic ordering temperature T_N

A sudden decrease due to antiferromagnetic ordering is observed in $\rho(T)$ as shown in Fig. 1(b). The antiferromagnetic ordering temperature T_N was defined as the minimum in the temperature dependence of second derivative of $\rho(T)$ since T_N at ambient pressure (T_N=3.8 K) in this work is in agreement with that obtained by neutron-scattering experiment (T_N=3.8 K).[13] The temperature dependence of $d^2\rho(T)/dT^2$ is shown in the inset of Fig. 2(a).

The pressure dependence of T_N is shown in Fig. 2(a). T_N decreases slightly up to 2 GPa as pressure increases and decreases rapidly above 2 GPa. Considering that the anomaly

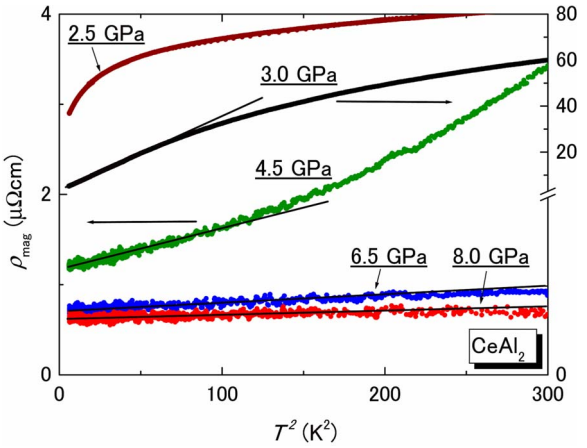

FIG. 3. (Color online) T^2 dependence of ρ_{mag} under high pressure.

in the $\rho(T)$ due to antiferromagnetic ordering becomes unclear above 2.5 GPa, T_N may disappear above 2.5 GPa. It has been reported that the positive pressure coefficient of T_N is predicted using the data of thermal-expansion measurement[23] in which T_N shows a maximum around 0.5 GPa and then T_N is decreased by applying higher pressure. However, T_N in the present work decreases as pressure increases without any peak in the pressure dependence. More experimental data are settled this point. The pressure where T_N=0 is obtained to be 2.7 GPa by a smooth extrapolation of the data as shown by dotted curve which indicates that QCP in $CeAl_2$ exists around 2.7 GPa.

C. Temperature dependence of the electrical resistivity around QCP

As was mentioned in Sec. III B, the pressure-induced QCP is considered to be observed around 2.7 GPa. In order to investigate the detailed behavior of $\rho(T)$ at low temperature below 2 K, we have measured $\rho(T)$ down to 50 mK, which is shown in Fig. 5. $\rho(T)$ changes significantly as pressure increases: the $\rho(T)$ at 2.1 GPa has a broad peak around 4 K followed by a rapid decrease below that due to magnetic

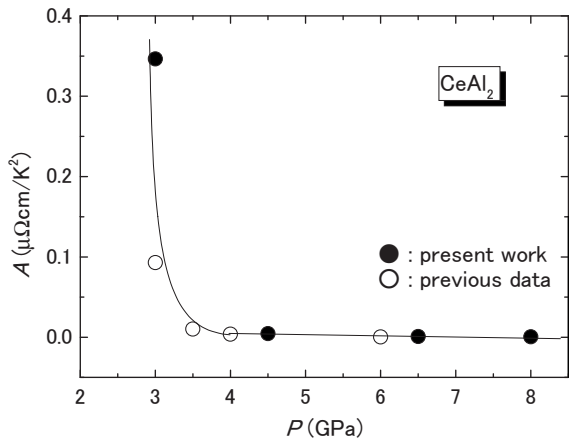

FIG. 4. Pressure dependence of the coefficient A of T^2. The solid line is a guide to the eyes.

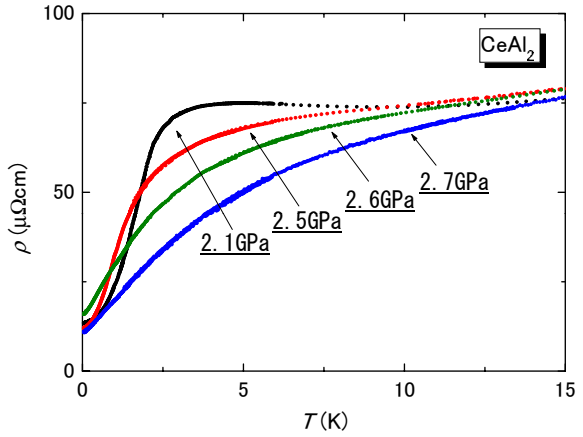

FIG. 5. (Color online) $\rho(T)$ under high pressure down to 50 mK.

ordering, but as pressure increases, the peak disappears and then $\rho(T)$ above 2.6 GPa shows a smooth increase with temperature. $\rho_{\mathrm{mag}}(T)$ is shown in Fig. 6. At 2.1 GPa, a peak is observed around 5 K. T_1 becomes unclear above 2.5 GPa and the shoulder is observed. Figures 1(b) are in good agreement within experimental error.

In some Ce compounds, the superconductivity has been observed around QCP,[3,24] which are known as the unconventional superconductivity such as d or p wave superconductivities. In the present work, no superconductivity was observed down to 50 mK at 2.7 GPa. Recently, it has been reported that the superconductivity is induced around P_v by valence fluctuation, where P_v is the pressure showing it. Since P_v of $CeAl_2$ may be higher than 2.7 GPa, a valence fluctuation mediated superconductivity is expected at higher pressure than 3 GPa.

D. Magnetoresistance under high pressure

Figure 7 shows the electrical resistivity $\rho(H)$ at 4.2 K as a function of magnetic field H under high pressure. Extremely large MR is observed, in which ρ is decreased about 40% by applying 9 T. All $\rho(H)$ curves show smooth change against

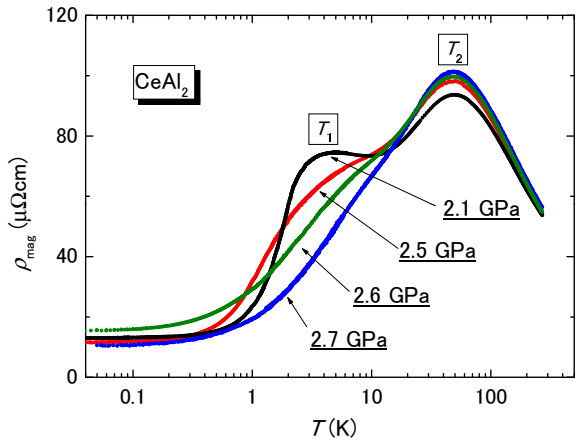

FIG. 6. (Color online) $\rho_{\mathrm{mag}}(T)$ at high pressure in the range $2.1 \leq P \leq 2.7$ GPa.

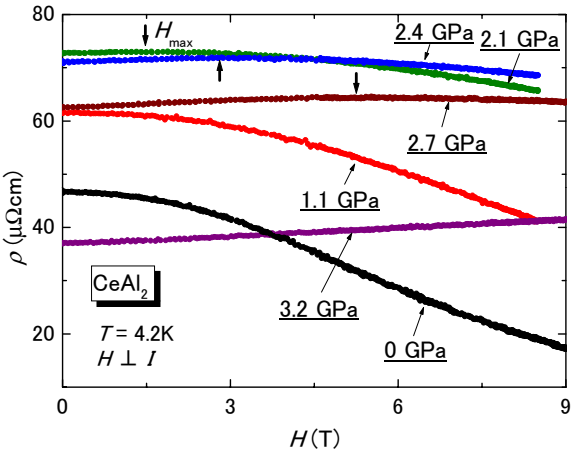

FIG. 7. (Color online) The electrical resistivity as a function of magnetic field.

H. This is due to the fact that no metamagnetic transition is observed at 4.2 K because the antiferromagnetic ordering occurs at 3.8 K at ambient pressure. Below 1.1 GPa, negative MR is observed up to 9 T, while at 2.1, 2.4, and 2.7 GPa, MR is positive at low magnetic field followed by a broad maximum around H_{max}, which is determined as the magnetic field of $d\rho/dH=0$ as shown in Fig. 8. $\rho(H)$ at 3.2 GPa shows a positive MR up to 9 T. Figure 8 shows the H dependence of the first derivative of $\rho(H)$, $d\rho/dH$. At ambient pressure, the values of $d\rho/dH$ show a minimum around 5 T, which indicates that MR tends to saturate above 5 T. At 1.1 GPa, the values of $d\rho/dH$ decrease up to 8.5 T without any minimum and the change of sign at H_{max} is observed around 1.5 T at 2.1 GPa. H_{max} shifts to high magnetic field as pressure increases, which is not observed up to 9 T at 3.2 GPa. Thus the sign of MR in $CeAl_2$ changes from negative to positive at high pressure. In order to examine the change of the resistivity by applying H, the values of $d\rho/dH$ are plotted in Fig. 9 as a function of pressure at $H=3$, 6, and 8.5 T. The signs of $d\rho/dH$ are found to change around 2.5, 2.7, and 2.9 GPa, respectively, which indicate that a crossover in the electronic state takes place around these pressures.

Negative MR indicates the incoherent Kondo state but positive MR indicates the coherent one.[25] Although 4.2 K is

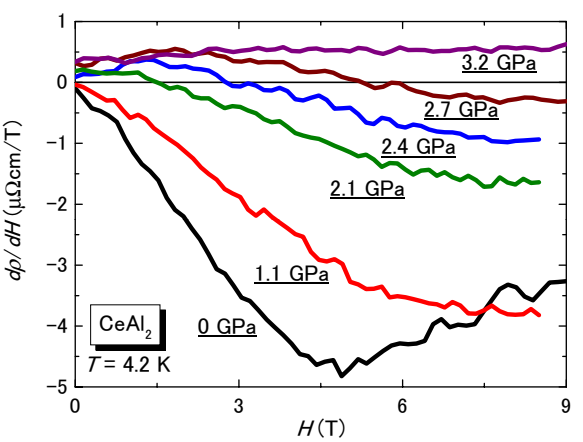

FIG. 8. (Color online) The magnetic-field dependence of first derivative of $\rho(H)$.

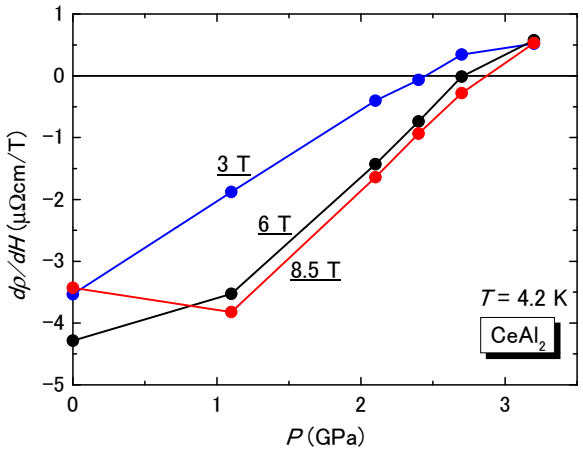

FIG. 9. (Color online) Pressure dependence of the value of $d\rho/dH$ at 3, 6, and 8.5 T.

below $T_K=6$ K, the electronic state in $CeAl_2$ at 4.2 K and ambient pressure is considered not to be stabilized as the coherent Kondo state. The mechanism of MR of heavy fermion substances has been explained on the basis of the periodic Anderson model by Kawakami and Okiji.[26] They calculated MR on the Ce substances as a function of H/T_K at various temperatures T/T_K. According to their results, the reduction of T/T_K induces the change from negative to positive MR. In this work, T/T_K decreases with increasing pressure since positive MR becomes stable at high pressure above 2.1 GPa. The reduction of T/T_K corresponds to an increase of T_K since T is constant (4.2 K) in the present work. The coherent Kondo state is considered to be stable above 3.2 GPa and 4.2 K since positive MR is observed without a maximum. The change from negative MR to positive MR is explained as a crossover from the incoherent Kondo state to the coherent one with increasing T_K.

IV. DISCUSSION

A. Effect of pressure on the Kondo scattering

T_1 decreases below 2.1 GPa as shown in Fig. 2(a). In general, T_1 in the concentrated Kondo substance corresponds roughly to T_K. Although T_K of $CeAl_2$ increases with pressure as indicated by the result described in D of Sec. III, T_1 below 2.1 GPa decreases. The antiferromagnetic order with spin-density wave is observed around 3.8 K at ambient pressure. Since SDW has a large effect on the electrical resistance and T_K is close to T_N, T_1 is influenced not only by Kondo effect but also by SDW. The reduction of T_1 may be connected to a decrease of T_N at high pressure. In other words, it appears that an increase of T_1 or T_K is masked by a decrease of T_N. However, T_1 begins to increase above 2.1 GPa. In $CeAl_2$, the coexistence of the sinusoidally modulated SDW phase and the simple type-II antiferromagnetic phase below 1.5 GPa has been reported. Above 2.0 GPa, SDW disappears and only the simple type-II antiferromagnetic phase exists.[13,14] The sudden change of T_1 around 2.1 GPa is due to disappearance of SDW, and T_1 is influenced only by Kondo effect above 2.1 GPa.

The Kondo temperature in the substance having two CEF splitting energies was calculated by using periodic Anderson model.[27] In this model, T_K is modified by CEF splitting and $\rho_{mag}(T)$ shows two maxima at T_K and T_K^h. T_K^h is described as follows:

$$T_K^h = (\Delta_1 \Delta_2 T_K)^{1/3}, \tag{1}$$

where Δ_1 and Δ_2 are the CEF splitting energies. T_K at ambient pressure is 6 K and magnitude of the CEF splitting is obtained to be $\Delta_1=100$ K and $\Delta_2=180$ K by the inelastic neutron scattering.[16] By using these values and Eq. (1), T_K^h is estimated to be 48 K, which is comparable with $T_2=62$ K. Although T_K increases at high pressure, T_2 decreases below 3 GPa. Thus the fact implies that the value of $\Delta_1\Delta_2$ decreases with pressure. Above 3 GPa, the peak corresponding to T_1 merges with that of T_2 and then the $\rho_{mag}(T)$ shows a single peak.

The $\rho_{mag}(T)$ in Fig. 1(b) shows $-\log T$ dependence in the two temperature ranges at ambient pressure, $7\ \mathrm{K} \leq T \leq 20$ K and $100 \leq T \leq 300$ K, which is a characteristic behavior of Kondo effect. The coefficients of $-\log T$ are defined to be m_1 and m_2 at low and high temperatures, as shown in Fig. 1(b). From the model presented by Cornut and Coqblin[28] (C-C),$\rho_{mag}(T)$ is described by the following equation:

$$\rho_{mag}(T) = \frac{3m^2\pi v_0 c}{e^2\hbar^3 k_F^2}\left[A + 2J_{sf}^2 D(\varepsilon_F)\frac{\lambda^2-1}{2j+1}\ln\frac{k_B T}{W}\right], \tag{2}$$

where A is the constant, c the cerium concentration, λ is equal to the total degeneracy of the $4f$ level, W is the cutoff energy, and other parameters have literal meaning. The degeneracy factor at low and high temperatures is defined as λ_L and λ_H, respectively. m_2/m_1 is written as

$$\frac{m_2}{m_1} = \frac{\lambda_H^2 - 1}{\lambda_L^2 - 1}. \tag{3}$$

Since the sixfold degenerate levels of Ce^{3+} ion are split by CEF effect into doublet and quartet in Ce compounds with cubic structure, the degeneracy factors λ_L for ground state and λ_H for thermally excited state are 2 and 6, respectively, i.e., $m_2/m_1=35/3\sim12$ from Eq. (3). m_2/m_1 in the present work is obtained $43/9\sim5$ at ambient pressure by the data in Fig. 1(b), which is smaller than the theoretical value. The value of m_2/m_1 in the previous data is almost the same as that in the present result.[29,30] Taking into account that $m_2/m_1=5$ and the ground state is a doublet, λ_H should be 4.[14] This supports that the CEF splitting in $CeAl_2$ is three levels, which is in agreement with the results obtained by neutron scattering.[16]

In Eq. (2), λ, W, and k_f are almost constant but a change in J_{sf} and $D(\varepsilon_F)$ at high pressure are dominant variation of m_1 and m_2, and these are related to J_{sf} and $D(\varepsilon_F)$ as follows:

$$m_1 \propto m_2 \propto |J_{sf}^2 D(\varepsilon_F)|. \tag{4}$$

The pressure dependence of m_1 and m_2 is shown in Fig. 10. Both m_1 and m_2 at low pressure increase with pressure, but they show a peak around 2 and 3 GPa, respectively. The pressure showing the peak of m_1 corresponds to that where

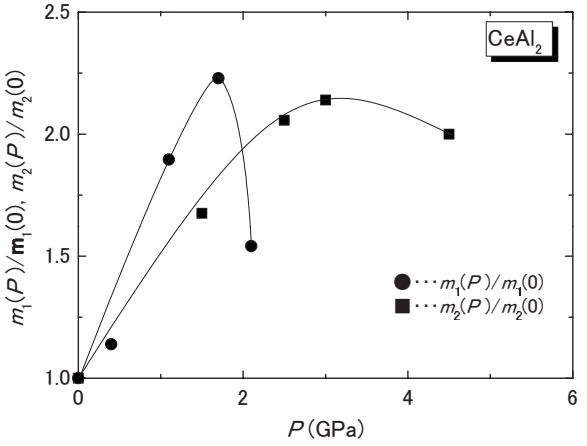

FIG. 10. m_1 and m_2 as a function of P.

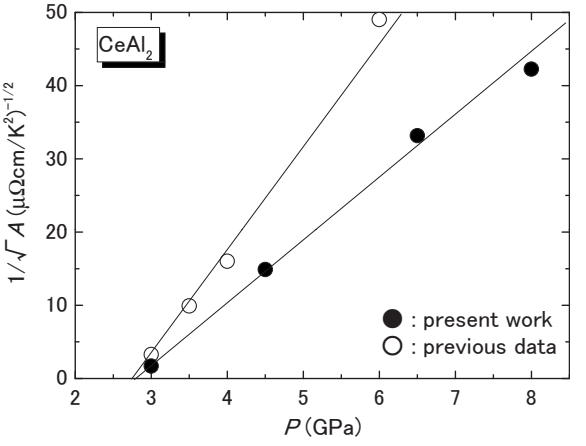

FIG. 12. $1/\sqrt{A}$ as a function of pressure.

the pressure derivative of T_1 changes from negative to positive as shown in Fig. 2(a). This fact implies that T_1 and m_1 are affected by the disappearance of SDW around 2 GPa. On the other hand, the pressure dependence of m_2 shows a peak around 3 GPa and the pressure corresponds well to that showing QCP. This may be due to the change of the electronic state around QCP, but the details of the origins are not known at present.

B. Grüneisen parameter of T_K and CEF splitting energy

Next we consider the present results in connection with Grüneisen parameter of T_2. Since T_2 corresponds to T_K^h, the Grüneisen parameter for T_K^h, Γ_K^h is written as follows:[31]

$$\ln\left[\frac{T_K^h(P)}{T_K^h(0)}\right] = \ln\left[\frac{T_2(P)}{T_2(0)}\right] = -\Gamma_K^h \ln\frac{V}{V_0}, \tag{5}$$

where V and V_0 are the volume at high and ambient pressures. Figure 11 shows the plot of $\ln[T_2(P)/T_2(0)]$ versus $-\ln(V/V_0)$. The two linear relationships are found as shown by the two solid lines and the values of Γ_K^h are −8 below 3 GPa and 33 above 3 GPa, respectively. Γ_K^h is also described by using Eq. (1) as follows:

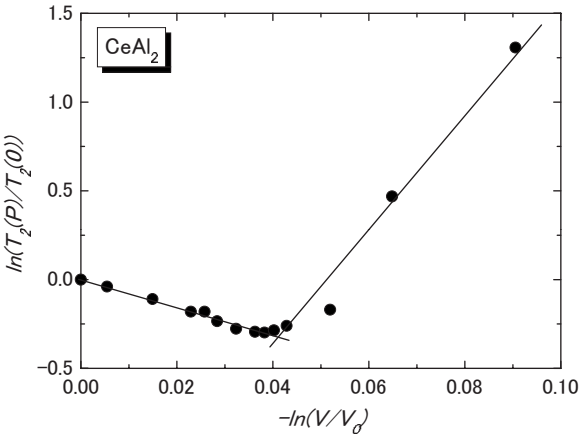

FIG. 11. $[T_2(P)/T_2(0)]$ as a function $-(V/V_0)$ in logarithmic scale.

$$\Gamma_K^h = -\frac{1}{3}\frac{\partial \ln \Delta_1}{\partial \ln V} - \frac{1}{3}\frac{\partial \ln \Delta_2}{\partial \ln V} - \frac{1}{3}\frac{\partial \ln T_K}{\partial \ln V} = \frac{2}{3}\eta + \frac{1}{3}\Gamma_K, \tag{6}$$

where η is the Grüneisen parameter of crystalline field splitting energy. Here we assume $\eta = -\partial \ln \Delta_1/\partial \ln V = -\partial \ln \Delta_2/\partial \ln V$. The value of Γ_K in $CeAl_2$ is 34.[32] Below 3 GPa, η is estimated to be −29, which indicates that the magnitude of CEF splitting decreases with increasing pressure. Above 3 GPa, Γ_K^h and Γ_K are almost the same. This result suggests that T_2 above 3 GPa, where a single peak is observed, corresponds to T_K and the degeneracy relevant to T_K changes from twofold to four- or sixfold.

C. Pressure-induced QCP

The coefficient A of T^2 term shown in Fig. 6 is related to T_K as $T_K \propto 1/\sqrt{A}$.[33] Figure 12 shows $1/\sqrt{A}$ as a function of pressure. Since $1/\sqrt{A}$ increases linearly with pressure, T_K increases at high pressure. $1/\sqrt{A}$ is found to be extrapolated to 0 around 2.7 GPa, which indicates that a phase boundary exists around $P_C \sim 2.7$ GPa. The previous result is also plotted in Fig. 12 for comparison.[7] The pressure of $1/\sqrt{A}=0$ coincides each other. Since the divergence in the magnitude of A or $T_K=0$ corresponds to a quantum phase transition (QPT), this result indicates that the QPT takes place at 2.7 GPa. This is supported by the results obtained in the following paragraph.

The electronic state near QCP is different from the normal Fermi-liquid behavior showing T^2 dependence in the electrical resistivity. Here we attempted to fit the present data illustrated in Fig. 6 to the following equation:

$$\rho_{mag} = \rho_0 + A_n T^n, \tag{7}$$

where ρ_0 and n are the residual resistivity and exponent connecting with electronic state, respectively.

$\rho_{mag}(T)$ below 2 K is shown in Fig. 13. Fitting was carried out in the temperature range 50 mK$\leq T \leq$2 K. Solid curves in Fig. 13 show the result of fitting, in which these curves reproduce well the experimental data. Figure 14 shows the pressure dependence of ρ_0 and n. ρ_0 has a peak around 2.7

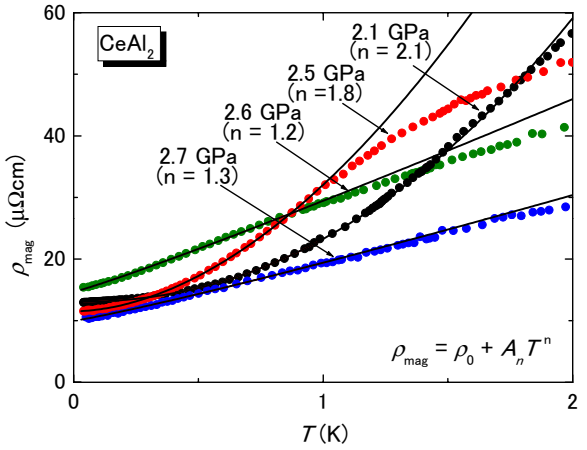

FIG. 13. (Color online) $\rho_{mag}(T)$ below 2 K under high pressure. Solid curves show the results of fitting.

GPa. n is 2 below 2 GPa but around 2.7 GPa, it is 1.3 ~1.4, which significantly deviates from the normal Fermi-liquid behavior ($n=2$). Judging from these facts, we conclude that $CeAl_2$ shows the QPT around 2.7 GPa. This indicates that the electronic state around 2.7 GPa is the so-called non-Fermi-liquid state. Furthermore, n becomes 2 above 3 GPa by applying pressure more as shown in Fig. 3, indicating that Fermi-liquid behavior is recovered.

D. $P-T$ phase diagram in $CeAl_2$

Finally, we make an attempt to construct the P-T phase diagram for electronic and magnetic states of $CeAl_2$ on the basis of the present data. Figure 15 shows the pressure dependence of the electrical resistivity at several temperatures

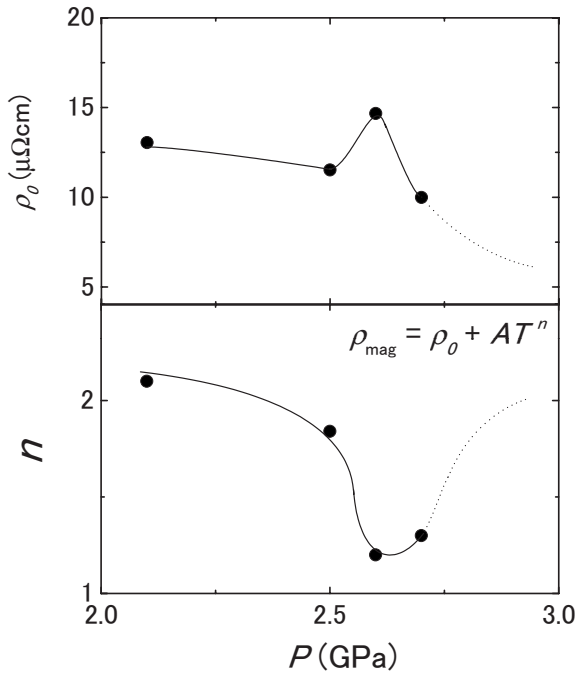

FIG. 14. ρ_0 and n as a function of pressure. The solid curves are drawn as guide to the eyes.

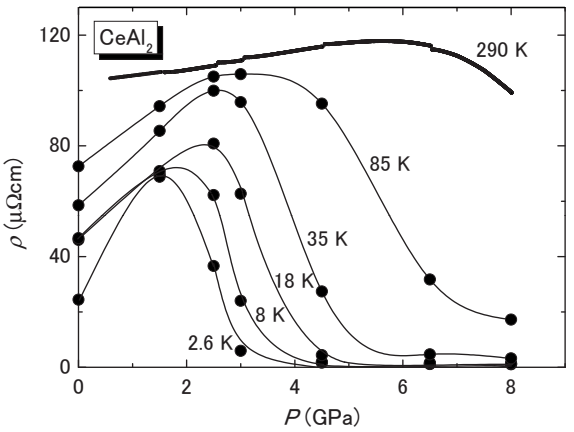

FIG. 15. Pressure dependence of the electrical resistivity at several temperatures. The full circles are obtained by isobaric temperature dependent data at several pressures. The thick line shows isothermal pressure dependence of the electrical resistivity at 290 K. Small discontinuities are observed in $\rho(P)$ curve due to technical reasons, which does not affect the results in the present work.

in the range 2.6 K$\leq T\leq$300 K which was obtained from the results in Fig. 1(a). For all the isothermal ρ-P curves, ρ increases with pressure followed by a maximum at $P=P_{max}$ and P_{max} increases with temperature. The maximum seems to be clear at low temperature ($T\leq$35 K) but to become broad at high temperature ($T\geq$85 K). It has been reported that there is a crossover induced by pressure from weak Kondo to strong Kondo regime, which is largely different from the first-order γ-α phase transition in Ce metal.[34] In such a sense, the peaks observed in Fig. 16 may correspond to the crossover in the electronic state of $CeAl_2$. P_{max}-T curve indicates that the Kondo temperature T_K increases with increasing pressure. P_{max} is plotted in Fig. 16. P_{max} increases gradually up to 2.6 GPa and rapidly above the pressure where T_2 also shows a similar change and then crosses room temperature at 5.5 GPa.

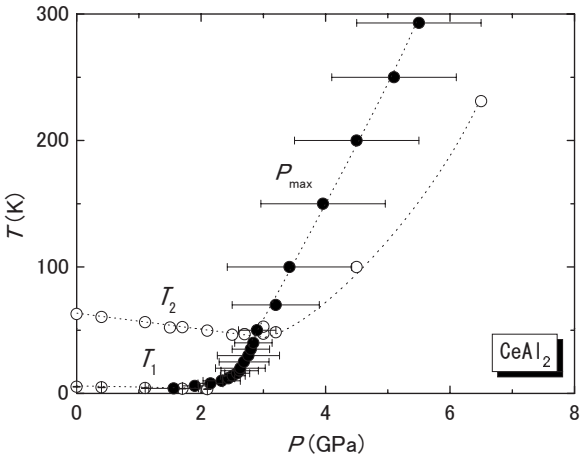

FIG. 16. P-T phase diagram obtained from the present data. The closed circles show the pressure P_{max} showing the maximum of ρ-P curves as shown in Fig. 15. The open circles show the pressure dependence of T_1 and T_2 for comparison with P_{max}.

V. CONCLUSION

The electrical resistivity of $CeAl_2$ has been measured in detail at high pressures. The $\rho(T)$ of $CeAl_2$ is changed dramatically by applying pressure. According to the analysis of pressure dependence of MR using Okiji-Kawakami model, T_K is found to increase with pressure. T_N is decreased by applying pressure and expected to disappear around 2.7 GPa. Since the coefficient of T^2 term diverges around 2.7 GPa, the magnetic phase boundary exists at 2.7 GPa. Non-Fermi-liquid behavior in $\rho(T)$ was observed around 2.7 GPa. Above 3 GPa, Fermi-liquid behavior was recovered. The pressure effect on T_2 changes around 3 GPa. Although $CeAl_2$ shows the QCP around 2.7 GPa, the superconductivity was not observed around 2.7 GPa above 50 mK.

[1] F. Steglich, J. Magn. Magn. Mater. **100**, 186 (1991).
[2] S. Doniach, Physica B & C **91**, 231 (1977).
[3] For the summary of recent progress in this research field, see J. Phys. Soc. Jpn. **76** (2007) Suppl., edited by T. Kagayama, M. Ohashi, and Y. Uwatoko.
[4] A. T. Holmes, D. Jaccard, and K. Miyake, Phys. Rev. B **69**, 024508 (2004).
[5] G. Knebel, D. Braithwaite, P. C. Canfield, G. Lapertot, and J. Flouquet, Phys. Rev. B **65**, 024425 (2001).
[6] G. R. Stewart, Rev. Mod. Phys. **73**, 797 (2001).
[7] G. Oomi, M. Ohashi, Y. Uwatoko, I. Satoh, and T. Komatsubara, Physica B **359-361**, 65 (2005).
[8] H. Miyagawa, M. Ohashi, G. Oomi, I. Satoh, and T. Komatsubara, Physica B **378-380**, 771 (2006).
[9] H. Miyagawa, Y. Fuchizaki, M. Ohashi, G. Oomi, I. Satoh, and T. Komatsubara, High Press. Res. **26**, 503 (2006).
[10] M. Ohashi, G. Oomi, S. Koiwai, M. Hedo, and Y. Uwatoko, Phys. Rev. B **68**, 144428 (2003).
[11] F. Steglich, C. D. Bredl, M. Loewenhaupt, and K. D. Schotte, J. Phys. Colloq. **C5**, 301 (1979).
[12] C. D. Bredl, F. Steglich, and K. D. Schotte, Z. Phys. B **29**, 327 (1978).
[13] B. Barbara, M. F. Rossignol, J. X. Boucherle, J. Schweizer, and J. L. Buevoz, J. Appl. Phys. **50**, 2300 (1979).
[14] B. Barbara, M. F. Rossignol, J. X. Boucherle, and C. Vettier, Phys. Rev. Lett. **45**, 938 (1980).
[15] S. Tomisawa, S. Wada, M. Ohashi, and G. Oomi, J. Phys.: Condens. Matter **18**, 10413 (2006).
[16] M. Loewenhaupt, B. D. Rainford, and F. Steglich, Phys. Rev. Lett. **42**, 1709 (1979).
[17] P. Thalmeier and P. Fulde, Phys. Rev. Lett. **49**, 1588 (1982).
[18] T. Sawamura, T. Andoh, G. Oomi, and Y. Ōnuki, Rev. High Pressure Sci. Technol. **7**, 614 (1998).
[19] C. Probst and J. Wittig, J. Magn. Magn. Mater. **9**, 62 (1978).
[20] F. Honda, S. Kaji, I. Minamitake, M. Ohashi, G. Oomi, T. Eto, and T. Kagayama, J. Phys.: Condens. Matter **14**, 11501 (2002).
[21] N. Môri, H. Takahashi, and N. Takeshita, High Press. Res. **24**, 225 (2004).
[22] D. Jaccard and A. T. Holmes, Physica B **359-361**, 333 (2005).
[23] R. Schefzyk, W. Lieke, and F. Steglich, Solid State Commun. **54**, 525 (1985).
[24] N. D. Mathur, F. M. Grosche, S. R. Julian, I. R. Walker, D. M. Freye, R. K. Haselwimmer, and G. G. Lonzarich, Nature (London) **394**, 39 (1998).
[25] A. Sumiyama, Y. Oda, H. Nagano, Y. Ōnuki, K. Shibutani, and T. Komatsubara, J. Phys. Soc. Jpn. **55**, 1294 (1986).
[26] N. Kawakami and A. Okiji, J. Phys. Soc. Jpn. **55**, 2114 (1986).
[27] K. Hanzawa, K. Yamada, and K. Yoshida, J. Magn. Magn. Mater. **47-48**, 357 (1985).
[28] B. Cornut and B. Coqblin, Phys. Rev. B **5**, 4541 (1972).
[29] M. Nicolas-Francillon, A. Percheron, J. C. Achard, O. Gorochov, B. Cornut, D. Jerome, and B. Coqblin, Solid State Commun. **11**, 845 (1972).
[30] Y. Ōnuki, Y. Furukawa, and T. Komatsubara, J. Phys. Soc. Jpn. **53**, 2734 (1984).
[31] T. Kagayama, G. Oomi, K. Iki, N. Mori, Y. Ōnuki, and T. Komatsubara, J. Alloys Compd. **213-214**, 387 (1994).
[32] G. Oomi, T. Kagayama, Y. Ōnuki, H. Mitamura, and T. Goto, in *Proceedings of the Moscow International Symposium on Magnetisum (MISM'99)*, Moscow, 1999 (Faculty of Physics, M. V. Lomonosov Moscow State University, Moscow), p. 351.
[33] A. Yoshimori and H. Kasai, J. Magn. Magn. Mater. **31-34**, 475 (1983).
[34] B. Barbara, J. Beille, B. Cheiato, J. M. Laurant, M. F. Rossignol, A. Waintal, and S. Zemirli, Phys. Lett. **113A**, 381 (1986).